

ratio. It is interesting to note that the five injection ranges appeared in Figs. 2 and 3 are also apparent in Figs. 4-7. In the low-injection linear range, most of the gold centers are in the thermal-equilibrium configuration and the lifetime is constant. In the quadratic range, the charge in the gold centers changes and most of these become neutral in the upper end of the range. The decrease of the lifetime is mostly due to the increase in hole density. In the intermediate linear range the distribution of charge in the gold centers and the lifetime are essentially constant. In the high-injection region the charge distribution changes to the high-injection linear range values and the electron lifetime again reaches a constant value. It is also noted from Figs. 6 and 7 that the normalized electron lifetime τ_n/τ_n^0 versus injection (Δn) depends strongly on the ratio of τ_n^0 and τ_p^0 .

V. CONCLUSIONS

The Shockley-Read and the Sah-Shockley statistics were used to describe the interaction of gold and phosphorus centers with injected carriers in silicon. The most significant effect of these centers on the injected electron and hole densities is that their equality is destroyed by the charge-balance requirement. The

relationship between the injected carriers for charge neutrality is established in the form of power laws (i.e., $\Delta p = \Gamma \Delta n^\alpha$) that hold in different ranges of injection.

The power-law relationship between Δp and Δn is linear (i.e., $\alpha=1$) in three ranges: at very low or very high injection and in an intermediate injection range. The low and intermediate ranges are joined by a well-defined quadratic range (i.e., $\alpha=2$). We have found the constants Γ and α that define these power laws in four defined ranges of injection. Also, numerical analysis was used to plot Δp versus Δn for all injections satisfying the neutrality condition (Figs. 2 and 3). Application of the present theory to the photomagnetolectric effect in gold-doped silicon at low temperatures has shown good agreement with experimental observation.⁵ Another application of the present theory to the diffusion of photoexcited carriers in semiconductors will be reported in a later publication.

ACKNOWLEDGMENT

This research was supported by the Advanced Research Projects Agency, U.S. Department of Defence and monitored by the Air Force Cambridge Research Laboratories under Contract No. F 19628-68-C-0058.

* Present address: Bell Telephone Laboratories, Inc., Allentown, Pa. 18103.

¹ W. Shockley and W. T. Read, Jr., Phys. Rev. **87**, 835 (1952).

² C. T. Sah and W. Shockley, Phys. Rev. **109**, 1103 (1958).

³ J. M. Brown and A. G. Jordan, J. Appl. Phys. **37**, 337 (1966).

⁴ J. Blakemore, *Semiconductor Statistics* (Pergamon, New York, 1962).

⁵ J. Agraz-G and S. S. Li, Phys. Rev. B **2**, 1847 (1970).

⁶ J. M. Fairfield and B. V. Gokhale, J. Solid State Electron. **8**, 685 (1965).

High-Field Distribution Function and Mobility in *n*-Type Cadmium Sulphide

S. GUHA

Solid State Electronics Group, Tata Institute of Fundamental Research, Bombay-5, India

(Received 27 March 1970)

The energy distribution function of carriers in *n*-type cadmium sulphide is calculated considering acoustic (both deformation-potential and piezoelectric), impurity, and polar optical modes of scattering. The drift velocity obtained from a rigorous solution of the Boltzmann equation is compared with the high-carrier-concentration case where strong carrier-carrier scattering imposes a displaced Maxwellian distribution on the carriers.

I. INTRODUCTION

The transport properties of *n*-type cadmium sulphide at high electric fields have received the attention of several workers.¹⁻⁵ The scattering process in this semiconductor is quite complex; in addition to the electron-electron and electron-ionized-impurity scattering, the carriers also interact with the acoustic phonons (both deformation- and piezoelectric-potential modes) and the polar optical phonons. In materials of low resistivity the application of a high electric field results in an appreciable disturbance in the acoustic-phonon distribu-

tion. This gives rise to an acoustoelectric current,⁶ which flows in a direction opposite to the normal drift current and gives rise to current saturation and oscillation when the applied field exceeds a certain critical value. For higher-resistivity materials, however, the phonons remain in equilibrium, and the experimental results should be explained satisfactorily by conventional hot-electron theory neglecting the acoustoelectric effect.

Hot-carrier conduction phenomena in semiconductors can be studied theoretically by solving the Boltzmann

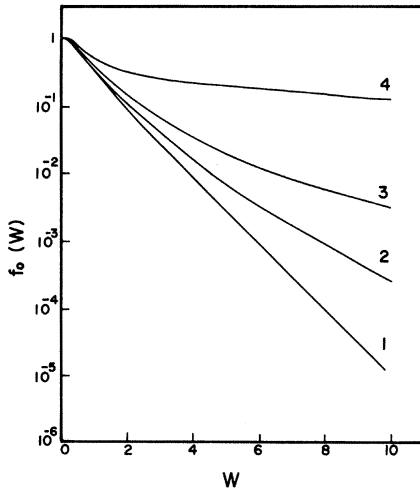


FIG. 1. Distribution function as a function of reduced energy for applied fields of (1) 10 kV cm⁻¹, (2) 20 kV cm⁻¹, (3) 50 kV cm⁻¹, and (4) 100 kV cm⁻¹.

transport equation taking into account the different scattering processes. The task is not simple because of the complexity of the scattering processes involved and simplifying assumptions are usually made. There have been two major ways of attack⁷: (i) In the first method, it is assumed that carrier concentration is sufficiently small so that one is justified in neglecting carrier-carrier scattering. The energy distribution function is then obtained by solving the Boltzmann equation taking into consideration the other scattering processes and the conductivity characteristic is obtained therefrom. (ii) In the second method, the carrier concentration is considered to be very large, so that the carriers share both their energy and momentum mainly amongst themselves. The distribution function in this case is Maxwellian, with an elevated effective temperature, displaced in the momentum space and the displacement and the effective temperature are obtained by solving the energy and the momentum balance equations.

Hot-carrier theory was first applied to *n*-type CdS by Onuki and Shiga¹ who considered a Maxwellian distribution for the carriers and scattering due to deformation- and piezoelectric-potential phonons only. A more rigorous theory involving the solution of Boltzmann equation considering the same types of scattering was developed by Saitoh.² Recently Crandall^{3,4} has tried to explain his experimental results on hot-carrier transport in CdS at different temperatures by developing a similar theory which takes into account impurity scattering too. Calculations of galvanomagnetic coefficients along similar line have also been done by Sodha and Sharma.⁵ All these authors have neglected polar optical-phonon scattering although the results of Saitoh and Crandall indicate that even at moderately high fields the average energy of the carriers would be

increased above the optical-phonon energy resulting in optical-phonon emission. The above theories would therefore be applicable strictly to low-temperature and low-field ranges. The purpose of the present paper is to develop a comprehensive hot-electron theory in CdS taking into account the different scattering mechanisms. To assess the sensitivity of the hot-carrier conduction characteristic to the shape of the energy distribution function, both the low- and the high-concentration models would be considered. In Sec. II the distribution function is derived by solving the Boltzmann equation taking into account the different scattering processes, and an expression for mobility is obtained therefrom. The high-concentration case is considered in Sec. III and equations giving the carrier temperature and mobility as a function of electric field are obtained assuming a displaced Maxwellian distribution. The numerical results obtained for the two cases are presented in Sec. IV and the implications of the results discussed.

II. HOT-CARRIER DISTRIBUTION FUNCTION AND MOBILITY

The Boltzmann equation in the steady state is given by

$$(\partial f / \partial t)_F + (\partial f / \partial t)_C = 0, \quad (1)$$

where $(\partial f / \partial t)_F$ and $(\partial f / \partial t)_C$ represent the rate of change of the distribution function due to the applied field and the different sources of scattering, respectively.

The energy distribution function of the carriers may be expanded in terms of Legendre polynomials as

$$f = f_0 + f_1 \cos \theta, \quad (2)$$

where θ is the angle between the wave vector \mathbf{K} and the

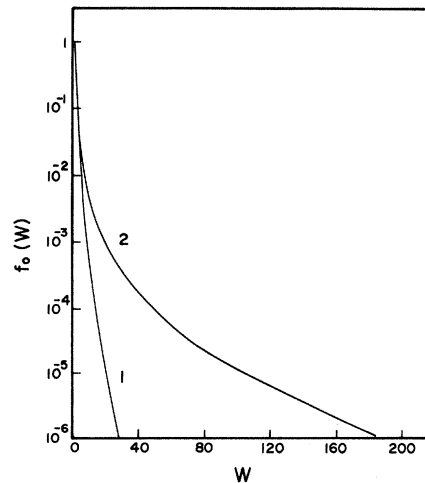


FIG. 2. Distribution function as a function of reduced energy for applied fields of (1) 30 kV cm⁻¹ and (2) 50 kV cm⁻¹.

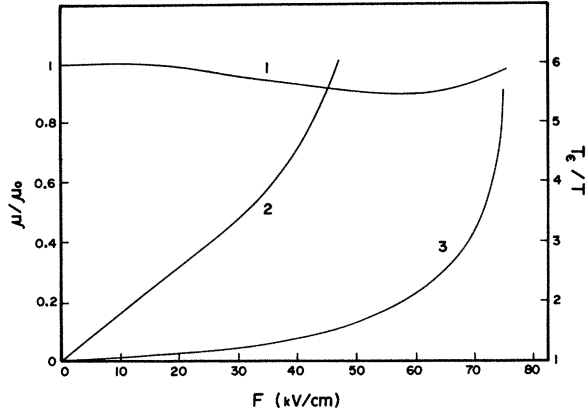


FIG. 3. Normalized mobility and carrier temperature as a function of applied field in the displaced Maxwellian model: (1) normalized mobility against field for 300°K, (2) normalized carrier temperature against field for 77°K, and (3) normalized carrier temperature against field for 300°K.

applied field \mathbf{F} . In writing Eq. (2) we have considered terms only up to the first order in the polynomial expansion. This is the diffusion approximation which is true only when the scattering is elastic so that the drift energy is much smaller than the thermal energy. In n -type cadmium sulphide, polar optical-phonon scattering, which is strongly inelastic, is predominant, and the above approximation would be valid only when the field is high enough to raise the average carrier energy much higher than the optical-phonon energy. However, since there is always elastic scattering present in the form of acoustic and impurity scattering which prevents any streaming action and randomizes the distribution, the quasielastic approximation made in writing Eq. (2) would not be in much error even for lower electric fields.⁸

On evaluating the scattering integrals making use of Eq. (2), one may separate the symmetric and asymmetric parts of the collision integrals as follows:

$$(\partial f_0 / \partial t)_{dp} = \frac{4(2m\hbar)\omega^{1/2}m^2\Xi^2}{\pi\hbar^4\rho} W^{1/2}[(W/2x_0)f_0'' + (\frac{1}{2}W + x_0^{-1})f_0' + f_0], \quad (3)$$

$$(\partial f_0 / \partial t)_{po} = \frac{2eF_0W^{-1/2}}{(2m\hbar\omega)^{1/2}[\exp(x_0) - 1]} \{ \sinh^{-1}W^{1/2}[\exp(x_0)f_0(W+1) - f_0] + \sinh^{-1}(W-1)^{1/2}[f_0(W-1) - \exp(x_0)f_0] \}, \quad (4)$$

$$(\partial f_1 / \partial t)_{dp} = -f_1 / \tau_{dp} = -f_1(2\hbar\omega/m)^{1/2}(m^2\Xi^2kT/\pi\hbar^4\rho S^2)W^{1/2}, \quad (5)$$

$$(\partial f_1 / \partial t)_{pe} = -f_1 / \tau_{pe} = -f_1(m/2\hbar\omega)^{1/2}(e^2kT\bar{v}_j^2/2\pi\hbar^2\epsilon_S^2\rho S^2)W^{-1/2}, \quad (6)$$

$$(\partial f_1 / \partial t)_{im} = -f_1 / \tau_{im} = -f_1W^{-3/2} \frac{\pi e^4 N_I \ln[1 + (\epsilon_S/e^2 N_I^{1/3})^2 \hbar^2 \omega^2 W^2]}{(2m\hbar\omega)^{1/2} \hbar \omega \epsilon_S^2}, \quad (7)$$

$$(\partial f_1 / \partial t)_{po} = -\frac{eF_0W^{-1/2}}{(2m\hbar\omega)^{1/2}[\exp(x_0) - 1]} \left\{ 2 \sinh^{-1}W^{1/2}f_1 - \exp(x_0)f_1(W+1) \left[\frac{(2W+1) \sinh^{-1}W^{1/2}}{W^{1/2}(W+1)^{1/2}} - 1 \right] \right. \\ \left. + 2f_1 \sinh^{-1}(W-1)^{1/2} \exp(x_0) - f_1(W-1) \left[\frac{(2W-1) \sinh^{-1}(W-1)^{1/2}}{W^{1/2}(W-1)^{1/2}} - 1 \right] \right\}, \quad (8)$$

where $W = \epsilon/\hbar\omega$ and $x_0 = \hbar\omega/kT$. ϵ is the carrier energy, $\hbar\omega$ is the optical phonon energy, m is the effective mass, ρ is the density, Ξ is the deformation potential energy, \bar{v}_j^2 is the piezoelectric constant, S is the sound velocity, ϵ_S is the static dielectric constant, and N_I is the ionized impurity density. F_0 has the magnitude of field and is given by

$$F_0 = (e\hbar\omega m/\hbar^2)(\epsilon_\alpha^{-1} - \epsilon_S^{-1}),$$

where ϵ_α is the high-frequency dielectric constant. The suffices dp , pe , im , and po refer, respectively, to deformation potential, piezoelectric, impurity and polar-optical modes of scattering. We have not considered the $(\partial f_0 / \partial t)$ terms for the piezoelectric and impurity scattering since these collision processes are elastic and do not contribute to the energy-loss mechanism. There is about 10% mass anisotropy in CdS which results in an anisotropy in the mobility of the order of 5%. For simplicity in the analysis we have neglected this anisotropy in the effective-mass values. Since we are essentially considering the transport phenomena at high fields and high temperatures, the anisotropy in the piezoelectric scattering is also neglected.

$(\partial f / \partial t)_F$ can also be similarly separated into symmetric and asymmetric parts to get a coupled differential equation for the solution of f_0 and f_1 . A solution of this equation is still extremely difficult unless one makes the relaxation-time approximation for the polar-optical modes which will be true at room temperature only when carrier energy is much larger than the optical-phonon energy. In such a case Eq. (8) reduces to

$$(\partial f_1 / \partial t)_{po} = -f_1 / \tau_{po} = -f_1 [eF_0 / (2m\hbar\omega)^{1/2}] [\exp(x_0) + 1] / [\exp(x_0) - 1] W^{-1/2}. \quad (9)$$

Expanding $f_0(W \pm 1)$ and neglecting the higher-order terms, one may eliminate f_1 from Eqs. (3)–(9) to get the following equation for f_0 :

$$(2e^2F^2/3m\hbar\omega)W^{-1/2}(d/dW)(W^{3/2}\tau f_0') + 2aW^{-1/2}(d/dW)[((2x_0)^{-1})W^2f_0' + \frac{1}{2}W^2f_0] \\ + bW^{-1/2}(d/dW)\{\frac{1}{2}[\exp(x_0)+1/\exp(x_0)-1](\ln 4x)f_0' + \ln 4xf_0\} = 0, \quad (10)$$

where

$$2a = 4(2m\hbar\omega)^{1/2}m^2\Xi^2/\pi\hbar^4\rho, \quad b = eF_0/(2m\hbar\omega)^{1/2}, \quad \text{and} \quad \tau = 1/(\tau_{dp}^{-1} + \tau_{pe}^{-1} + \tau_{im}^{-1} + \tau_{po}^{-1}).$$

One thus obtains

$$f_0 = N_a \exp - \int_0^W \left[\frac{(aW^2 + b \ln 4W)dW}{(a/x_0)W^2 + \frac{1}{2}b\{\exp(x_0)+1\}/\{\exp(x_0)-1\} \ln 4W + (2e^2F^2/3m\hbar\omega)W^{3/2}\tau} \right] \\ = N_a \exp \left(- \int_0^W h(W)dW \right). \quad (11)$$

N_a is the normalization constant given by

$$N_a = \frac{2\pi^2\hbar^3/(2m\hbar\omega)^{3/2}}{\int_0^\alpha W^{1/2} \exp[-\int_0^W h(W)dW]dW}. \quad (12)$$

One may now evaluate the current density as a function of field from the relation

$$J = \frac{ne\hbar}{m} \int_0^\alpha K \cos\theta f_1 \cos\theta d\mathbf{K} \\ = \frac{2}{3} \frac{ne^2}{m} F \frac{\int_0^\alpha \exp[-\int_0^W h(W)dW]h(W)\tau W^{3/2}dW}{\int_0^\alpha W^{1/2} \exp[-\int_0^W h(W)dW]dW}. \quad (13)$$

III. ENERGY AND MOMENTUM BALANCE CONDITIONS FOR DISPLACED MAXWELLIAN CASE

When the carrier concentration is large, the carriers share both their energy and momentum mainly amongst themselves and the distribution function is then given by

$$f = A \exp - (\hbar^2 |\mathbf{K} - \mathbf{K}_0|^2 / 2mkT_\epsilon), \quad (14)$$

where $\hbar K_0$ is the displacement in the momentum space. $\hbar K_0$ and T_ϵ may be obtained by solving the energy and momentum balance conditions given by

$$\int_0^\alpha \epsilon \left[\left(\frac{\partial f}{\partial t} \right)_F + \left(\frac{\partial f}{\partial t} \right)_C \right] d\mathbf{K} = 0, \quad (15)$$

$$\int_0^\alpha \mathbf{K} \left[\left(\frac{\partial f}{\partial t} \right)_F + \left(\frac{\partial f}{\partial t} \right)_C \right] d\mathbf{K} = 0. \quad (16)$$

On substituting the values of $(\partial f/\partial t)_F$ and $(\partial f/\partial t)_C$, and integrating term by term, one obtains the following coupled equation giving μ , the mobility as a function field:

$$\mu^{-1} = \frac{4m}{3e\sqrt{\pi}} \left\{ \frac{2}{a_1} x_e^{-1/2} + b_1^{-1} x_e^{1/2} + c_1^{-1} x_e^{3/2} I \right. \\ \left. + \frac{eF_0 x_e^{3/2} \exp(\frac{1}{2}x_e) [K_0(\frac{1}{2}x_e) [\exp(x_0 - x_e) - 1] + K_1(\frac{1}{2}x_e) [\exp(x_0 - x_e) + 1]]}{2(2m\hbar\omega)^{1/2} [\exp(x_0) - 1]} \right\}, \quad (17)$$

$$\mu F^2 = (8m/e\sqrt{\pi})(S^2/a_1)x_0^{-1/2}x^{3/2}(1-x^{-1}) + (F_0/\sqrt{\pi})[\exp(x_0) - 1]^{-1} (2\hbar\omega/m)^{1/2} x_e^{1/2} \exp(\frac{1}{2}x_e) K_0(\frac{1}{2}x_e) [\exp(x_0 - x_e) - 1], \quad (18)$$

where

$$x = T_\epsilon/T, \quad x_e = \hbar\omega/kT_\epsilon, \quad a_1 = \tau_{dp}W^{1/2}, \quad b_1 = \tau_{pe}W^{-1/2},$$

$$c_1 = \tau_{im} \ln[1 + (\epsilon_S/e^2 N_I^{1/3})^2 \hbar^2 \omega^2 W^2] W^{-3/2},$$

and

$$I = \int_0^\alpha \frac{e^{-W} dW}{\ln[1 + (\epsilon_S/e^2 N_I^{1/3})^2 \hbar^2 \omega^2 W^2]}.$$

K_0 and K_1 are modified Bessel functions of the second kind. It should be mentioned that in deriving these integrals the relaxation-time approximation for the optical phonons has not been made.

IV. NUMERICAL RESULTS AND DISCUSSIONS

A. Low-Concentration Case

Equation (11) was integrated numerically to obtain the energy distribution function as a function of energy for different values of electric field. The following values of the parameters were assumed²:

$$\begin{aligned} m/m_0 &= 0.17, & \Xi &= 25.6 \times 10^{-19} \text{ J}, \\ \bar{e}_j^2 &= 0.3103 \text{ C}^2/\text{m}^4, & \rho &= 4.8 \times 10^8 \text{ kg/m}^3, \\ S &= 4.26 \times 10^8 \text{ m/sec}, & \hbar\omega/k &= 440^\circ\text{K}, \\ \epsilon_S/\epsilon_0 &= 9.19, & \epsilon_a/\epsilon_0 &= 5.24, \end{aligned}$$

and

$$N_T = 10^{15}/\text{cm}^3.$$

This gives a value of low-field mobility $\mu_0 = 273 \text{ cm}^2 \text{ V}^{-1} \text{ sec}^{-1}$ which agrees reasonably well with the experimental values. Equation (11) has a singularity at $W = 0$ and hence for values of W less than 0.3, f_0/N_a was considered to be equal to unity. This assumption will not give rise to much error in the derived mobility values since there are very few electrons in this range of energy.

Figure 1 shows the plot of the normalized distribution function as a function of reduced energy for different electric fields. For low fields, the distribution function is Maxwellian, but there is a significant departure from a Maxwellian distribution as the field is raised above 10 kV cm^{-1} . As compared with the Maxwellian distribution of the same average energy, it is observed that there are fewer low-energy electrons and relatively more higher-energy electrons. This results from the decreasing effectiveness of the polar optical scattering with increasing energy and has also been observed in other polar semiconductors.^{8,9} It should, however, be mentioned that because of the acoustic scattering present, which is negligible in the energy-loss process at low and intermediate energies, but extremely predominant at high carrier energies, the distribution function does converge even at very high electric fields. This is illustrated in Fig. 2, where the distribution function is plotted against energy for a field of 30 and 50 kV cm^{-1} . The high-energy tail of the distribution function is found to be considerably extended at high fields.

TABLE I. Variation of normalized carrier mobility with applied field.

Field (kV cm^{-1})	μ/μ_0
1	1
10	0.99
20	0.96
30	0.95
50	0.96
60	0.99

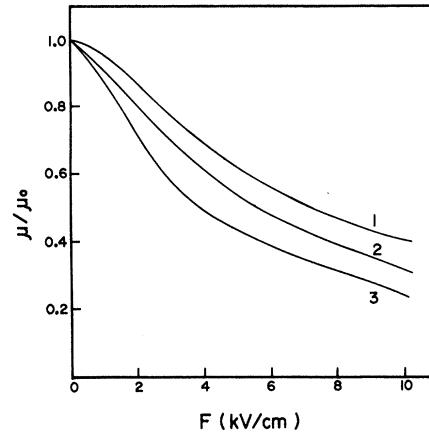


FIG. 4. Normalized mobility as a function of applied field at 77°K in the displaced Maxwellian model: (1) considering all the scattering processes, (2) with impurity scattering neglected, and (3) using parameters which fix low-field mobility at $4660 \text{ cm}^2 \text{ V}^{-1} \text{ sec}^{-1}$.

The field dependence of carrier mobility was obtained by calculating the integral in Eq. (13). The results are shown in Table I. It is observed that departure from Ohm's law is not appreciable even at very high fields. There is a small decrease in mobility with increasing field; for fields above 50 kV cm^{-1} the mobility starts increasing, a phenomenon typical in semiconductors with predominant optical-phonon scattering.

Because of the approximation involved in the theory, the analysis would not be valid for low temperatures. The results are hence presented for the temperature of 300°K only.

B. High-Concentration Case

Calculations were made for both 300 and 77°K and the results are shown in Figs. 3 and 4. The results are summarized below:

1. 300°K

The basic features of the mobility variation with electric field are identical to those obtained in the non-Maxwellian case. There is a decrease in mobility initially with increase in field; but for fields above 30 kV cm^{-1} the mobility starts increasing with field. The carrier temperature initially increases with field slowly; for fields above 60 kV cm^{-1} the increase is very rapid.

2. 77°K

(i) The mobility decreases with increase in field and departure from Ohm's law occurs at a much lower field. At 2.5 kV cm^{-1} , the mobility reduces to 80% of the low-field value; at 12.5 kV cm^{-1} it becomes about one-third.

(ii) The carrier temperature increases with electric field slowly up to 25 kV cm^{-1} , beyond which the increase is very rapid.

(iii) The effect of impurity scattering is to reduce

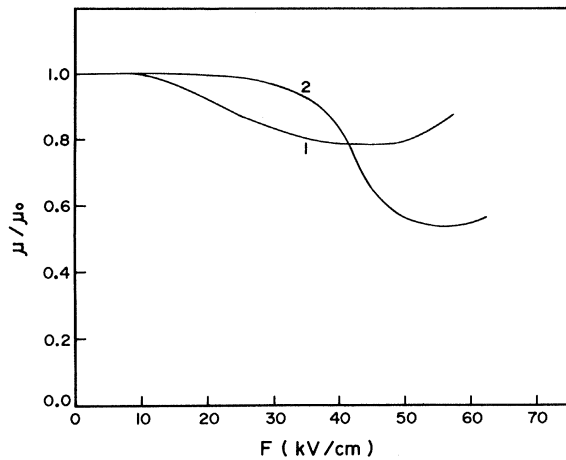


FIG. 5. Normalized mobility as a function of applied field at 230°K: (1) theoretical results and (2) experimental results of Boer and Bogus.

the value of low-field mobility. Heating effect and departure from Ohm's law therefore occurs at a much lower field when impurity scattering is neglected and the magnitude of deviation from linearity is also larger.

It should be mentioned that the values of the different parameters assumed fix the low-field mobility at $2600 \text{ cm}^2 \text{ V}^{-1} \text{ sec}^{-1}$; when the impurity scattering is neglected, the low-field mobility is $3200 \text{ cm}^2 \text{ V}^{-1} \text{ sec}^{-1}$. The experimental values for low-field mobility given in the literature vary between 2200 to $5000 \text{ cm}^2 \text{ V}^{-1} \text{ sec}^{-1}$. Calculations were also made with the following parameters: $m=0.15m_0$, $\Xi=20.5 \times 10^{-19} \text{ J}$ and $\bar{e}_2^2=0.2628 \text{ C}^2/m^4$ and with impurity scattering neglected. The above choice of parameters fixes the low-field value of acoustic and piezoelectric mobilities identical to those used by Crandall³ and a value of low-field mobility of $4660 \text{ cm}^2 \text{ V}^{-1} \text{ sec}^{-1}$. The results indicate that carrier heating takes place at a much lower field and there is significant departure from Ohm's law even at fields below 1 kV cm^{-1} .

The experimental data on hot-electron mobility available in the literature^{10,11} are influenced by the acoustoelectric interaction in the material and cannot be directly compared with the theoretical results presented here. Boer and Bogus¹² have recently measured the electric field dependence of Hall mobility in CdS at 230°K from an analysis of stationary cathode-adjacent high-field domains.¹³ The samples were biased in the range of differential negative conductivity and the Hall probes were placed in the region of the stationary domain where the electric field is approximately constant. It was not possible to change the field values in the domain in the same sample, and hence different crystals were used to obtain the field dependence of the mobility.

Calculations have been made for a temperature of 230°K with the set of parameters detailed above. The

low-field mobility value computed is $516 \text{ cm}^2 \text{ V}^{-1} \text{ sec}^{-1}$, which agrees well with the data available in the literature, but is somewhat lower than the value of $620 \text{ cm}^2 \text{ V}^{-1} \text{ sec}^{-1}$ obtained by Boer. The theoretical results are presented in Fig. 5 where the results obtained by Boer are also shown. It is observed that the results have the same qualitative features: a field-independent mobility up to a certain critical field strength, followed by a range of field strength where the mobility decreases with increase in electric field. At very high fields, mobility starts increasing with field as was the case at 300°K. The quantitative agreement between theory and experiment is however rather poor. The theory predicts deviation from Ohm's law due to hot-electron effects at much lower fields; at fields above 30 kV cm^{-1} , however, the dependence of mobility on field is found to be much larger in the case of the experimental values. The source of this discrepancy between theory and experiment is not very clear. The two-term spherical-harmonic approximation to the distribution function underestimates the inelasticity of the optical-phonon scattering process and allows the electrons to heat up more rapidly. This would result in the lowering of the mobility at a lesser field. At very high fields the assumption of the displaced Maxwellian distribution would result in an underestimate of the number of high-energy carriers, but this would not seriously affect the mobility values as borne out by our 300°K calculations. It should be mentioned that the theory gives the values of drift mobility whereas the experimental results are for Hall mobility, but in CdS these values are not much different.^{1,2} The use of different crystals to achieve different field strengths in the experiments could be a possible source of error and hence, till further experimental results are available it is not possible to ascertain definitely the cause for this discrepancy.

V. CONCLUSIONS

Hot-electron conduction in *n*-type cadmium sulphide is studied theoretically taking into account the different scattering mechanisms. The distribution function is derived by solving the Boltzmann equation and the conductivity mobility obtained therefrom. The results are found to agree with those obtained for the case when the distribution function is assumed to be a displaced Maxwellian one. This indicates that the magnitude of conductivity mobility is not very sensitive to the exact shape of the distribution function.

The results have been found to agree qualitatively with the experiments of Boer. The quantitative agreement however is rather poor. The other available experimental data are influenced by acoustoelectric interaction and cannot be directly compared with theory. It should be mentioned however that an acoustoelectric domain has a finite build-up time which ranges from 20 nsec to a few μsec , and if the experiment is performed with pulses having a duration smaller than

the build-up time, the effect of phonon disturbance can be eliminated and the results can be directly applied to theory. Experiments are in progress and will be reported in the near future.

ACKNOWLEDGMENT

The author is indebted to N. Subramanian for his help in programming the computations.

¹ M. Onuki and K. Shiga, J. Phys. Soc. Japan Suppl. **21**, 427 (1966).

² M. Saitoh, J. Phys. Soc. Japan **21**, 2540 (1966).

³ R. S. Crandall, Phys. Rev. **169**, 577 (1968).

⁴ R. S. Crandall, Phys. Rev. **169**, 585 (1968).

⁵ M. Sodha and S. Sharma, Phys. Status Solidi **30**, 239 (1968).

⁶ R. W. Smith, Phys. Rev. Letters **9**, 87 (1962).

⁷ See, for example, E. M. Conwell, in *High Field Transport in Semiconductors*, edited by F. Seitz, D. Turnbull and H. Ehrenreich

(Academic, New York, 1967).

⁸ E. M. Conwell and M. O. Vassel, Phys. Rev. **166**, 797 (1968).

⁹ D. Matz, Phys. Rev. **168**, 843 (1968).

¹⁰ A. R. Moore and R. W. Smith, Phys. Rev. **138**, A1250 (1965).

¹¹ P. G. Le Comber, W. E. Spear, and A. Weinstein, Brit. J. Appl. Phys. **17**, 467 (1966).

¹² K. W. Boer and K. Bogus, Phys. Rev. **176**, 899 (1968).

¹³ K. W. Boer and P. Voss, Phys. Rev. **171**, 899 (1968).

Recombination Parameters in Low-Resistivity Gamma-Irradiated *n*-Type Germanium*†

J. R. SROUR AND O. L. CURTIS, JR.

Northrop Corporate Laboratories, Hawthorne, California 90250

(Received 25 June 1970)

Detailed studies of recombination in $\sim 0.2\text{-}\Omega$ cm As- and Sb-doped Co^{60} γ -irradiated Ge are reported. The principal experimental techniques used were measurement of the variation of minority-carrier lifetime with temperature (at low excess density) and with excess density (using temperature as a parameter). The temperature dependence of the electron capture probability c_n was obtained for both dopant cases. The hole capture probability c_p was found, in both cases, to be approximately independent of temperature over the range examined. For Sb-doped material at 323°K, the recombination-center energy-level position (neglecting statistical weight) was found to be 0.361 ± 0.005 eV above the valence band, with a possible slight temperature dependence corresponding roughly to one-half the variation of the band gap with temperature. The capture-probability ratio c_p/c_n at this same temperature was 740. For the As-doped case, two different levels appear to dominate the recombination process in annealed and unannealed low-resistivity material. The energy-level positions relative to the valence band (neglecting statistical weight) are 0.327 ± 0.005 and 0.37 ± 0.01 eV at room temperature for the annealed and unannealed samples, respectively. The corresponding capture-probability ratios are 650 and 810. As in the case of Sb doping, the energy level appears to shift with temperature at about one-half the rate of the shift in band-gap energy.

INTRODUCTION

The properties of recombination and trapping centers introduced in *n*-type Ge by Co^{60} γ irradiation have been studied extensively.¹⁻⁷ Because of inherent experimental difficulties, however, very little work has been reported on low-resistivity ($\lesssim 0.5 \Omega$ cm) material. Studies in such material possess the potential of being particularly informative because of the comparative absence of trapping, and the comparative dominance in the expression for minority-carrier lifetime of a term whose only temperature dependence arises from capture-probability variation. Detailed recombination studies on low-resistivity As- and Sb-doped material are reported herein. A primary goal in studying material with high carrier concentration was to investigate in some detail capture-probability temperature dependences, and to obtain reliable information about the capture-probability ratio c_p/c_n . Coupled with data from higher-resistivity samples, this should yield accurate positions for energy levels associated with the radiation-induced defects.

The principal experimental techniques used were

measurement of the variation of minority-carrier lifetime with temperature (at low excess density) and with excess density (using temperature as a parameter). In the course of the study, improved techniques were developed for utilizing these concurrent measurements in the determination of recombination parameters.

EXPERIMENTAL

Measurements of minority-carrier lifetime as a function of temperature at low excess density were performed using experimental procedures described previously.⁸ The method involves observation of photoconductivity decays. Lifetime as a function of excess density, with temperature as a parameter, was measured using a modification of a method also described elsewhere.⁹ The Xe flash lamp previously used for photoexcitation of carriers was replaced by a steady-state light source (R.I. Controls model 5292 high-intensity infrared spot heater). Light to the sample was controlled by a hand-operated shutter, and excess density was varied by using different